

## Computational Study of Important Parameters in Deep Burn Modular Helium Reactor

Di Yun, Thomas A. Patten, Bei Ye, James F. Stubbins\*

*Department of Nuclear, Plasma and Radiological Engineering*

*University of Illinois at Urbana-Champaign, Urbana, Illinois 61801 USA*

### Abstract

We performed incineration capability modeling on the General Atomics Deep Burn Modular Helium Reactor design (DB-MHR) loaded with fuel manufactured from LWR waste. This paper focuses on several critical neutronic features of the fuel cycle such as neutron spectrums, one-group capture and fission cross-sections and fission to capture ratios of Pu-239. Their impacts on total transmutation capability of the reactor are studied. Different axial shuffling strategies are analyzed. The spatial self-shielding effect is also considered.

**KEYWORDS:** *TRISO, transmutation ratio, self-shielding effect, axial shuffling*

### 1. Introduction

This study examines the incineration capability optimization of the modular helium reactor (DB-MHR) that was conceived by General Atomics. The DB-MHR is helium cooled, graphite moderated reactor that provides benefits such as: high fuel burn-up, high plant efficiency, passive safety, flexible choice of fuel, and a fuel form highly resistant to failure at high burn-ups (TRISO) [1]. This paper investigates the use of reprocessed spent LWR fuel in the DB-MHR. The DB-MHR uses two types of fuel, driver fuel (DF) and transmutation fuel (TF). The DF contains Pu and Np in the form of  $NpPuO_{1.7}$  from spent LWR fuel and is irradiated for three fuel cycles. The initial composition of the fresh DF is shown in table 1. The DF contains most of the fissile material (Pu-239 and Pu-241), which is depleted through fission during use in the reactor. The TF contains spent DF with added Am and Cm from spent LWR fuel and is irradiated for three fuel cycles. The TF mostly contains non-fissile isotopes which are depleted through both capture and capture followed by fission during residence in the reactor. The TF also provides extra reactivity control. The objective of this study is to optimize the system overall transmutation ratio. The overall TRU (transmutation ratio) is the ratio of total transmuted actinides to the total actinides loaded to the system. The final TRU of the Pu-239 was determined to be able to reach as high as 95 % and all actinides to be as high as 62% in realistic reactor operation conditions making this an attractive method for destruction of LWR spent fuel. This research focused on maximizing the actinide destruction by examining the roles of fuel particle size, fuel re-loading mass, and fuel shuffling strategies (both axial and radial) on the TRU in the DB-MHR.

**Table 1:** Initial composition of the fresh DF

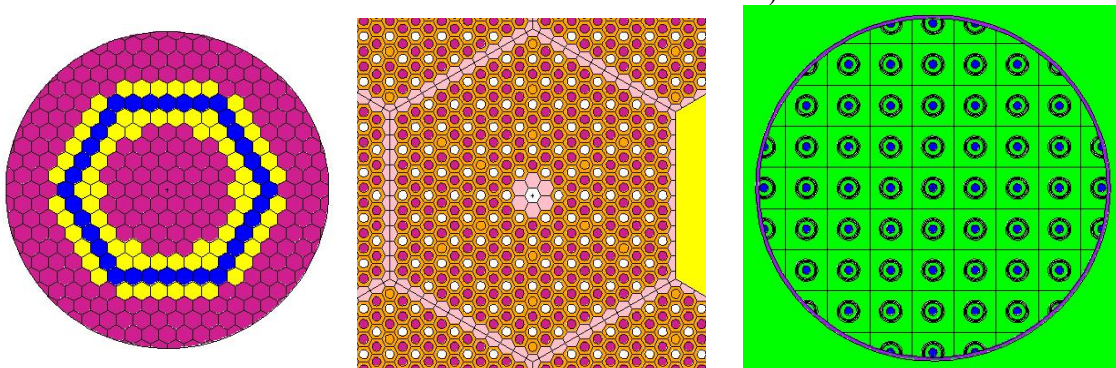
| Isotope | Mass percentage |
|---------|-----------------|
| Np-237  | 4.68            |
| Pu-238  | 1.34            |
| Pu-239  | 51.28           |
| Pu-240  | 20.71           |
| Pu-241  | 7.46            |
| Pu-242  | 4.34            |
| O-16    | 10.19           |

## 2. Description of the Deep Burn Modular Helium Reactor Model

The calculations for the DB-MHR were performed using a 3D full core model created in MCNP5 [2]. The cross-sections were from the JEF 2.2 library. The burn-up calculations were performed using MCNP5-MONTEBURNS-ORIGEN2. MONTEBURNS [3] couples the MCNP5 and ORIGEN2 [4] codes to calculate the depletion of the nuclear fuel. At each time step, the fuel composition,  $k_{eff}$ , neutron flux, and one-group cross sections are recalculated. Both the MCNP5 and ORIGEN2 codes have been well benchmarked though the Monteburns code linking the two is still in the early stages of benchmarking [5]. At each time step, 275,000 neutron histories were run.

The DB-MHR reactor consists of three separate fuel rings surrounding a center graphite moderator region. Each fuel ring contains 36 hexagonal fuel blocks. Each fuel block contains 144 DF channels and 72 TF channels each with a diameter of 0.622 cm. 108 coolant channels are also contained there, each with a diameter of 0.797 cm. Each fuel channel contains the fuel in TRISO fuel particles packed with graphite. The influence of the DF kernel diameter was modeled for three cases: 300 $\mu$ m, 500 $\mu$ m, and 800 $\mu$ m. The TF kernel size was taken to be 250 $\mu$ m in diameter. The TRISO particle consists of several layers designed to contain the fuel. [1]. Fig. 1 illustrates the cross section view of the geometry of the whole reactor, a fuel block and a DF fuel channel.

**Figure 1:** MCNP5 model of DB-MHR reactor geometry (cross section view of full core, a fuel block and a DF fuel channel)



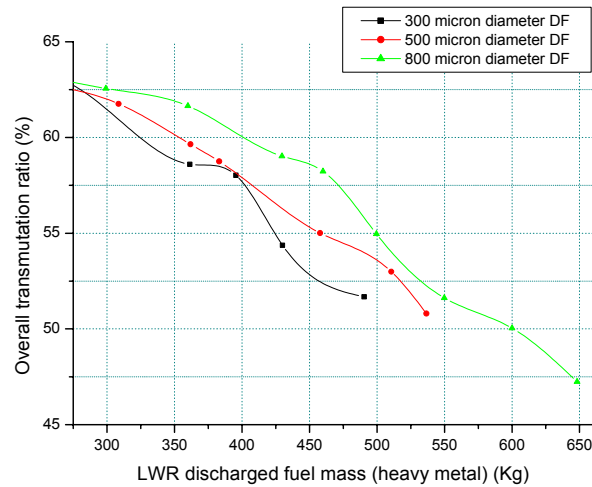
The reactor was run at 600 MWth for 12 fuel cycles. The 12th fuel cycle contains a fuel composition that has reached equilibrium. The time that the reactor was run for each fuel cycle varied with the loading mass of the fuel. This time was determined by the reactor being run until the  $k_{eff}$  reached just above 1. At the end of each fuel cycle, fresh DF is loaded in the middle fuel ring while older fuel is shuffled to the inner then outer ring. DF that is removed from the outer ring has the fission products removed and then is reprocessed with the  $AmCmO_{1.7}$  added and loaded in the middle fuel ring as fresh TF. The TF shuffling pattern is the same as the DF pattern. The resulting composition of the TF after its 3rd fuel cycle represents the waste composition that is deposited into a repository.

There are several sources of error in our model of the DB-MHR. First, the control rods were not put in the system. This is not expected to be a large source of error in the end of cycle fuel composition since the system is run close to critical [6]. The JEF 2.2 cross-section data library was used in this modeling. This data library includes the major fission products but lacks some of the more minor fission products. Using ENDF/B 6.8 or JENDL 3.2 data libraries in a similar model run for the DB-MHR can change the results as much as 3.5% in the burn-up results as reported in another work [7]. The temperature treatment of the reactor was run using cross-section data for 1500 K in the fuel and 1200 K in the graphite. A more detailed temperature analysis can improve the accuracy of the calculations. The volume used for the TF was taken to be half that of the DF in order to simplify the model. This resulted in an unrealistic density for the TF. Several cases were run in which the density of the TF was reduced to a realistic number. These cases did not show any significant impact on the final burn-up of the system.

### 3. Results and Discussions

#### 3.1 Reactor Overall Incineration Capability

The DB-MHR incineration capabilities have been investigated. Effects of two main parameters, reactor initial fuel loading mass and fuel kernel size, were studied. The initial fuel loading mass is a combined factor of both fuel kernel size and fuel packing fraction. Fig. 2 shows how the overall transmutation ratio (TRU) changes with initial fuel loading mass where DF kernel sizes were varied and TF kernel sizes were kept the same. It can be concluded that TRU decreases as the initial fuel loading mass increases and that TRU increases with fuel kernel size becoming larger. This shows that DB-MHR with larger driver fuel kernel has a better incineration capability. The advantage as is measured in the figure is in the range of 3% to 6% overall TRU. Both above effects can also be interpreted as a result of neutron spectrum change when the DF kernel size varies or the initial fuel loading mass changes. This issue will be addressed in the following section.

**Figure 2:** Overall TRU curves with different DF kernel sizes

### 3.2 Neutron Spectrums and Neutronic Features

In order to better understand the neutronic performance of DB-MHR which controls the reactor burn-up capability, we calculated the neutron spectra for all the cases above using MCNP5 with JEF2.2 cross-section library.

Fig.3 shows the neutron spectra averaged in all fuel particles in the reactor core at the beginning of 12th fuel cycle for different initial fuel loading mass. The DF kernel diameter was set at 300 $\mu$ m. The dips around 0.3eV and 1eV are caused by very large resonance capture cross-sections of Pu-239 and Pu-241 respectively. The dips become shallower with lower fuel initial loading mass because the concentrations of absorbing isotopes, Pu-239 and Pu-241 are both lower. It is seen from the figure that the thermal neutron flux is higher when the initial loading mass becomes lower due to the presence of smaller amount of actinides and therefore lower neutron absorptions. Both the one-group fission cross-section and radiative capture cross-section are then smaller. This is because the neutron fission cross-sections and radiative capture cross-sections of Pu-239, which is the most abundant fissile isotope that sustains criticality, are several orders of magnitude larger at thermal energies than at fast energies. By applying the Bateman equations, smaller one-group cross-sections contribute to the lower overall transmutation reaction rates. The harder spectrums also lead to lower fission to capture ratio of Pu-239 in DF as is demonstrated in **table 2**. A lower fission to capture ratio of Pu-239 yields smaller  $k_{eff}$  which, in turn, results in lower TRU.

**Figure 3:** Neutron spectrums averaged in all fuel particles in the reactor core at the beginning of 12<sup>th</sup> fuel cycle for different initial loading mass (300µm)

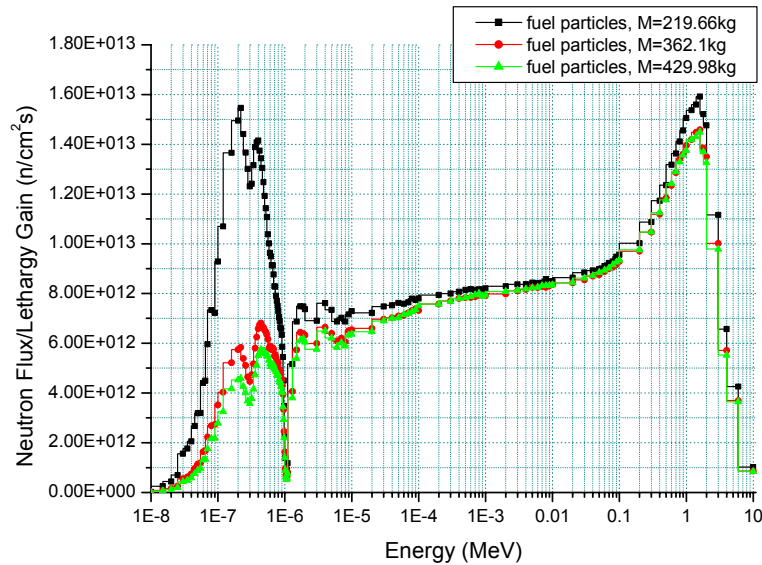


**Table 2:** Fission to capture ratio of Pu-239 (DF kernel diameter 300µm)

| Mass (kg) | 219.66 | 257.45 | 361.3  | 395.52 | 429.98 |
|-----------|--------|--------|--------|--------|--------|
| Inner DF  | 1.6392 | 1.6355 | 1.6316 | 1.6307 | 1.6255 |
| Middle DF | 1.6395 | 1.6304 | 1.6157 | 1.6146 | 1.6078 |
| Outer DF  | 1.6293 | 1.6260 | 1.6294 | 1.6212 | 1.6196 |
| Inner TF  | 1.6197 | 1.6185 | 1.6167 | 1.6133 | 1.6117 |
| Middle TF | 1.6168 | 1.6156 | 1.6039 | 1.6020 | 1.6006 |
| Outer TF  | 1.6221 | 1.6214 | 1.6196 | 1.6183 | 1.6160 |

Fig. 4 illustrates neutron spectra averaged in DF particles in the middle fuel ring at the beginning of 12th fuel cycle for three different DF kernel sizes: 300µm, 500µm and 800µm diameter, where the initial loading mass are kept constant at 360kg. Being the middle fuel ring, isotopic compositions are the same. The heterogeneity of the fuel particle is not considered here but will be addressed later separately. The case with larger DF kernel size has higher thermal because the redistributed graphite between fuel particles inside each fuel channel gives a better chance for neutron to slow down. These neutron spectra lead to both larger one-group fission and capture cross-sections and better fission to capture ratios in the DF regions for the case of larger DF kernel size. **Table 3** summarizes the one-group fission and capture cross-sections and fission to capture ratios in the DF regions for the two cases.

**Figure 4:** Neutron spectrums averaged in DF particles in the middle fuel ring at the beginning of 12<sup>th</sup> fuel cycle for different DF kernel sizes (M=360kg)

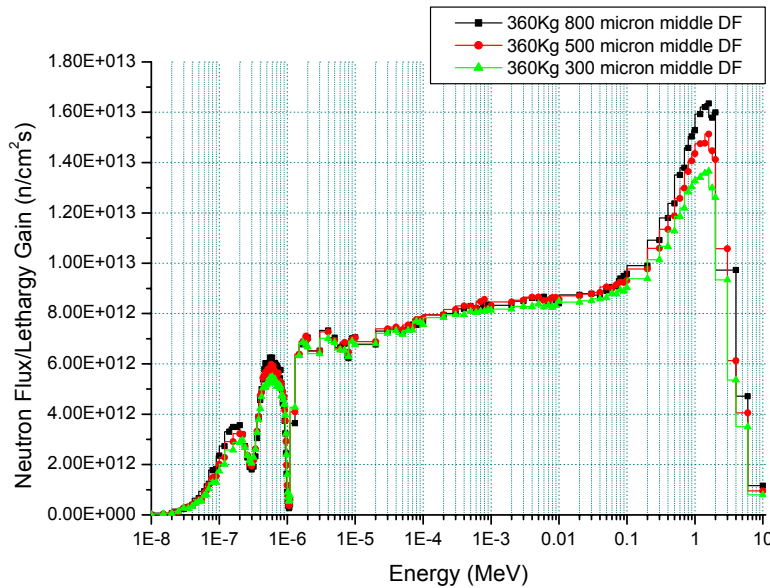


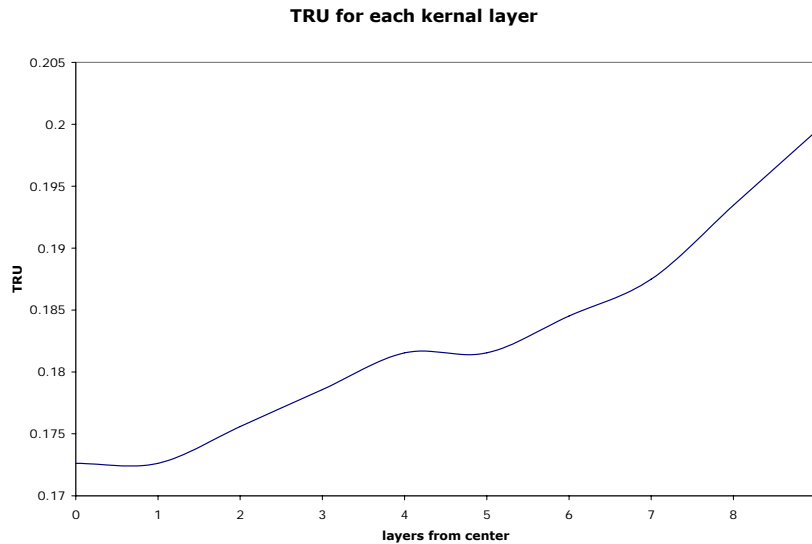
**Table 3:** Comparison of one-group capture and fission cross-section and fission to capture ratio of Pu-239

|                               | 300µm DF kernel |           |          | 500µm DF kernel |           |          | 800µm DF kernel |           |          |
|-------------------------------|-----------------|-----------|----------|-----------------|-----------|----------|-----------------|-----------|----------|
|                               | Inner DF        | Middle DF | Outer DF | Inner DF        | Middle DF | Outer DF | Inner DF        | Middle DF | Outer DF |
| 1-group capture cross-section | 41.0            | 25.8      | 64.2     | 45.7            | 29.2      | 70.3     | 48.3            | 31.6      | 78.1     |
| 1-group fission cross-section | 66.9            | 41.7      | 105      | 75.0            | 47.7      | 115      | 79.7            | 51.7      | 129      |
| Fission to capture ratio      | 1.6316          | 1.6147    | 1.6294   | 1.6427          | 1.6310    | 1.6323   | 1.6496          | 1.6375    | 1.6463   |

In the above discussions, the burn-up of transuranic actinides inside the TRISO particles was considered as homogeneous. However, the heterogeneity of the fuel particle introduces spatial self-shielding effect where the outer part of the fuel particle actually shield the inner part of the fuel particle. The very large resonance absorption cross-section of Pu-239 at 0.3eV provides a barrier at the outer layer of the fuel particle so that neutrons at this energy rarely reach inner part of the fuel particle. An improved fission to capture ratio is expected for the inner part of the particles. To this end, a very simple reactor model with fuel particles sliced into 10 equal volume layers was investigated where the reactor is loaded with just one type of fuel with a kernel diameter of 300µm. The reactor core volume was set to obtain a reasonable initial multiplication

factor. Incineration capabilities of each layer of the fuel particles were investigated using MonteBurns. Fig. 5 shows the calculated overall TRU in the different layers of the fuel particles after the fuel cycle. Results showed that outer layers were burned deeper than the inner layers. Although the expected improved fission to capture ratios were found in the inner layers, the general burn-up rates which are reflected by the one-group fission and capture cross-sections were much lower. This counteracting effect finally led to lower incinerations in the inner layers.

**Figure 5:** Overall TRU in different layers of fuel particles



To include more interacting factors to the heterogeneity study, another simulation was conducted where the whole DB-MHR was modeled. DF fuel kernel diameter was kept at 300 $\mu$ m, and was sliced into 5 equal volume layers. Fig. 6 compares neutron spectra of the five layers. The final overall transmutation ratios of each layer are illustrated in Fig. 7. Incineration capabilities of different layers vary as much as around 8% of total TRU with outermost layer the highest and innermost layer the lowest. Inner layers did show improved fission to capture ratios. However, under the influence of significantly lower one-group fission and capture cross-sections, inner layers present lower incineration capabilities. The overall TRU of the heterogeneous model is less than 1% lower than that of a comparable homogeneous model. As a result, homogenous fuel kernel models can be used reliably on overall reactor burn-up modeling.

**Figure 6:** Neutron spectrums averaged over five layers in middle DF region at the beginning of 12<sup>th</sup> fuel cycle (DF kernel diameter = 300 $\mu$ m, initial loading mass = 359.98kg)

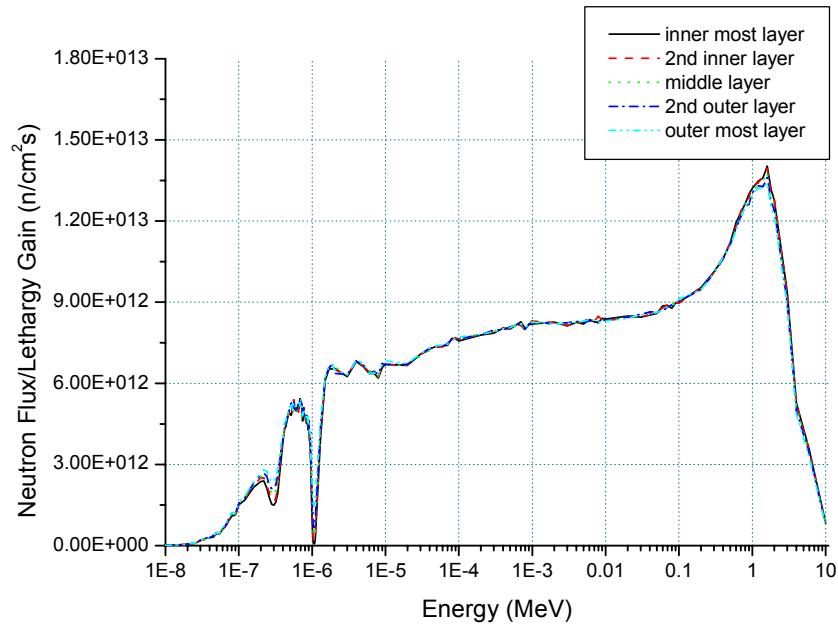
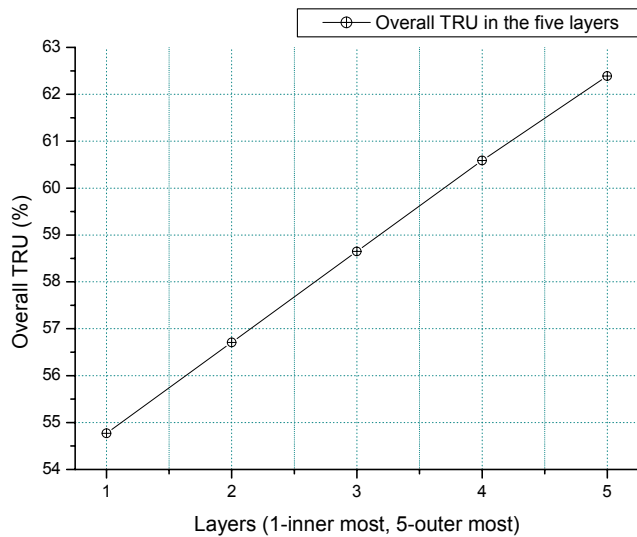


**Figure 7:** Overall transmutation ratio of the five layers in the fuel particles



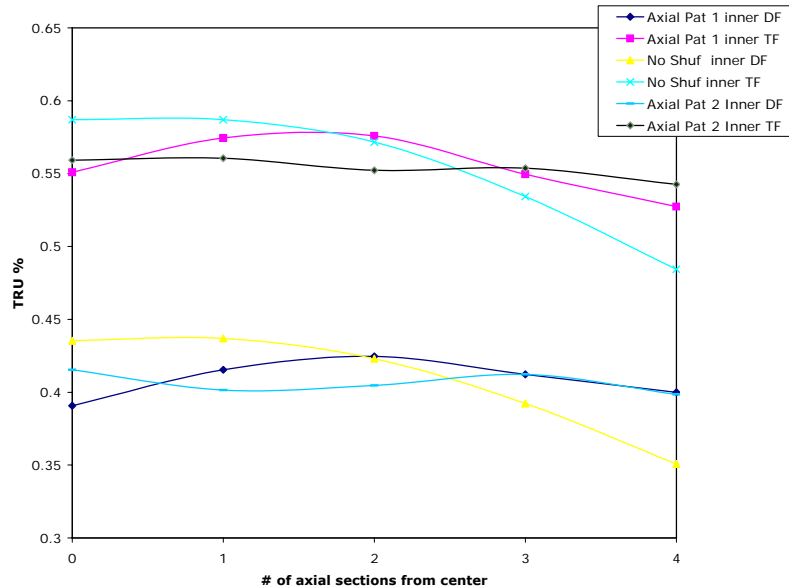
### 3.3 Axial Fuel Shuffling Strategies

Heterogeneity on the axial direction has been added by dividing the fuel channel into 10 fuel blocks. This is the actual geometry of the General Atomics design. Burn-up variation along the



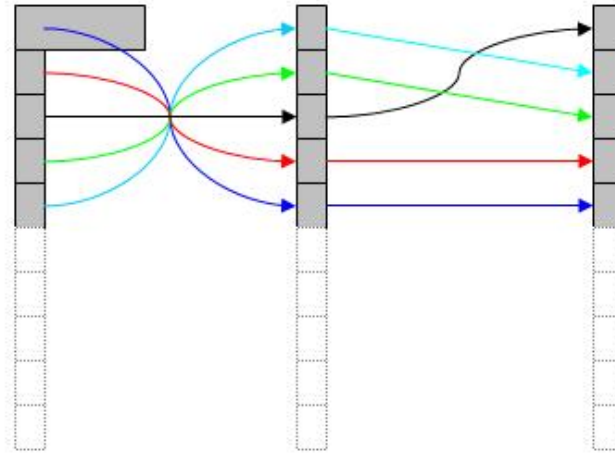
vertical axis can be seen in Fig. 8. Very little change was observed in the overall TRU, but a large variation was seen between the center and the top of the fuel channel. The end of cycle burn-up shows a variation as high as 9% of overall TRU.

**Figure 8:** Axial burn-up using different shuffling patterns for end of cycle DF and TF for 360kg loading mass



Two shuffling patterns were used trying to reduce the burn-up variation between the axial sections. Pattern #1 simply reversed the order of the fuel sections reflected over the center of the fuel pin each time the fuel was moved to a different layer of the reactor. This is also indicated as the axial shuffling strategy for the current reactor design. Pattern #1 reduced the burn-up variation between the axial sections to around 4% with the highest burn-up in the sections that started 2 sections from the center of the fuel channel. Pattern #2 was developed in an attempt to reduce the burn-up variation by shifting the section that received the greatest burn-up in the first shuffling pattern. This pattern is shown on Fig. 9. Using Pattern #2, the variation in the burn-up was reduced to 2%.

**Figure 9: Fuel shuffling pattern #2**



Little change was seen in the flux in each of the fuel regions while there was a noticeable change in the individual axial fluxes depending on the composition. This supports the conclusion that the total incineration of the system did not change from the non-shuffling case while the axial shuffling lead to a more even after cycle composition along the axial sections.

#### **4. Conclusion**

Detailed 3-D full-core simulations of the Deep Burn Modular Helium Reactor have been performed using the MCNP5-MONTEBURNS-ORIGEN2 codes. Reactor incineration capabilities were investigated.

A negative correlation was seen between reactor refueling mass and overall TRU and a positive correlation was seen between fuel kernel size and overall TRU. Reactors modeled with either larger refueling mass or smaller fuel kernel size have harder neutron spectrums leading to both lower one-group fission and capture cross-sections and lower fission to capture ratios.

The study of heterogeneous fuel particle model showed enhanced fission to capture ratios but lower burn-up ratios in the inner layers of the fuel particle. The overall TRU varies by less than 1% compared to the homogeneous model.

The use of axial shuffling strategies has little impact on overall transmutation ratio, but has significant impact on the burn-up along the axial sections. The variation in section burn-up can be reduced from 9% with no axial shuffling to about 2% utilizing an axial shuffling strategy.

#### **Acknowledgements**

This work was supported by the DOE-INIE Big 10 Consortium through DOE Contract Number 2406-UI-DOE-4423.

## References

- 1) A. Talamo, W. Gudowski, J. Cetnar, F. Venneri, Key Physical Parameters and Temperature Reactivity Coefficients of the Deep Burn Modular Helium Reactor Fueled with LWRs Waste, *Annals of Nuclear Energy*, 31, 1913-1937 (2004)
- 2) J.F. Briesmeister, MCNP- A General Monte Carlo N-Particle Transport Code, Version 4C, LANL-13709-M (2000)
- 3) D.I. Poston, H.R. Trellue, User's Manual, Version 2.0 for MonteBurns, Version 1.0, LA-UR-99-4999 (1999)
- 4) A.G. Croff, A User's manual for ORIGIN2 computer code, ORNL/TM-7175 (1980)
- 5) C. Trakas, L. Daudin, Benchmarking of MONTEBURNS against Measurements on Irradiated UOX and MOX Fuels, PHYSOR-2004 Topical Meeting on The Physics of Fuel Cycles and Advanced Nuclear Systems: Global Development, Chicago (2004)
- 6) C. Trakas, G. B. Bruna, Optimization of Deep-Burner-Modular Helium Reactor (DB-MHR) Concept for Actinides Incineration. American Nuclear Society Topical Meeting in Mathematics and Computations, Avignon, France (2005)
- 7) A. Talamo, W. Gudowski, J. Cetnar, Comparative Studies of ENDF/B-6.8 and JENDL-3.2 Data Libraries by Monte Carlo Modeling of High Temperature Reactors on Plutonium Based Fuel Cycle, *Journal of Nuclear Science and Technology*, vol 41, No. 12, 1228-1236 (2004)
- 8) M.A. Feltus, Overview of the DOE Advanced Gas Reactor Fuel Development and Qualification Program and Gas Reactor R&D, IAEA Technical Meeting on Current Status and Future Prospects of Gas Cooled Reactor Fuels, Vienna, Austria (2004)